



**HAL**  
open science

## **ZnO films formed by atomic layer deposition as an optical biosensor platform for the detection of Grapevine virus A-type proteins**

Alla Tereshchenko, Viktoriia Fedorenko, Valentyn Smyntyna, Igor Konup, Anastasiya Konup, Martin Eriksson, Rositsa Yakimova, Arunas Ramanavicius, Sébastien Balme, Mikhael Bechelany

### ► To cite this version:

Alla Tereshchenko, Viktoriia Fedorenko, Valentyn Smyntyna, Igor Konup, Anastasiya Konup, et al.. ZnO films formed by atomic layer deposition as an optical biosensor platform for the detection of Grapevine virus A-type proteins. *Biosensors and Bioelectronics*, 2017, 92, pp.763 - 769. 10.1016/j.bios.2016.09.071 . hal-01670214

**HAL Id: hal-01670214**

**<https://hal.umontpellier.fr/hal-01670214>**

Submitted on 15 Jun 2021

**HAL** is a multi-disciplinary open access archive for the deposit and dissemination of scientific research documents, whether they are published or not. The documents may come from teaching and research institutions in France or abroad, or from public or private research centers.

L'archive ouverte pluridisciplinaire **HAL**, est destinée au dépôt et à la diffusion de documents scientifiques de niveau recherche, publiés ou non, émanant des établissements d'enseignement et de recherche français ou étrangers, des laboratoires publics ou privés.

**ZnO films formed by atomic layer deposition as an optical biosensor platform for the detection of Grapevine virus A-type proteins**

Alla Tereshchenko<sup>1,\*</sup>, Viktoriia Fedorenko<sup>1,2</sup>, Valentyn Smyntyna<sup>1</sup>, Igor Konup<sup>3</sup>, Anastasiya Konup<sup>4</sup>, Martin Eriksson<sup>5</sup>, Rositsa Yakimova<sup>5</sup>, Arunas Ramanavicius<sup>6</sup>, Sebastien Balme<sup>2</sup>, Mikhael Bechelany<sup>2</sup>

<sup>1</sup> Faculty of Physics, Experimental physics department, Odessa National I. I. Mechnikov University, 42, Pastera, 65026, Odessa, Ukraine

<sup>2</sup> Institut Européen des Membranes IEMM, ENSCM UM CNRS UMR5635, Place Eugène Bataillon, F-34095 Montpellier Cedex 5, France

<sup>3</sup> Department of Microbiology, Virology and Biotechnology, Odessa National I. I. Mechnikov University, 2, Shampanskiy lane, 65000, Odessa, Ukraine

<sup>4</sup> National Scientific Centre “Institute of Viticulture and Wine Making Named After V. Ye. Tairov”, 27, 40 Let Pobedy str., 65496, Odessa, Ukraine

<sup>5</sup> Department of Physics, Chemistry and Biology, Linköping University, 58183 Linköping, Sweden

<sup>6</sup> Department of Physical Chemistry, Vilnius University, Naugarduko str. 24, LT-03225 Vilnius, Lithuania

**Abstract**

Novel sensitive optical biosensor **for the determination of Grapevine virus A-type (GVA) proteins (GVA-antigens) has been designed. This biosensor was** based on thin films of Zinc

oxide (ZnO) deposited by atomic layer deposition (ALD). The ZnO-based films have demonstrated favorable surface-structural properties for the direct immobilization of antibodies against GVA-antigens in order to form a biosensitive layer sensitive to GVA-antigens. The immobilization was confirmed by intensity changes in the main near band emission (NBE) peak of ZnO and by the formation of intense photoluminescence band, discovered in the visible range around 425 nm, caused by the immobilized proteins. The GVA-antigen detection was performed by the evaluation of changes and behavior of corresponding luminescence band. The sensitivity of as-formed label-free biosensor towards the GVA-antigens was determined in the range from 1 pg/ml to 10 ng/ml, in addition, the selectivity of biosensor was evaluated.

## Keywords

ZnO, Atomic layer deposition (ALD), Photoluminescence, Optical Biosensor, *Grapevine virus A-type*

## 1. Introduction

*Grapevine virus A-type* (GVA) is a type of grape leafroll viruses that is the most regularly detected virus in grapevine. Grape leafroll viruses are easily transmitted from infected to healthy plants during grafting and by insect pests common in vineyards. Vine-grapes infected with leafroll virus have poor health, poor-quality and low-yielding fruit (Du Preez et al., 2011; Goszczynski, 2014; Misbeh et al., 2007). Even if GVA virus was identified more than 30 years ago, it is still common in vineyards worldwide. In addition, its origin is relatively unknown and it has negative economic impact on vineyard productivity. Up to date the monitoring and diagnostics of GVA (as well as other types of leafroll viruses) are based on the study of its genome, genomic organization and replication mechanism (Du Preez et al., 2011; Misbeh et al., 2007). For example, complete genome sequence of a natural mutant of GVA was determined by

Goszczyński *et al.* (Misbeh *et al.*, 2007). However, up to date, the determination of GVA is based on serological methods (ELISA tests) and nucleic acid-based methods (variety of PCR approaches). These methods provide high sensitivity, up to 100 % detection, however they are time consuming, labour intensive and relatively expensive. Therefore, there is a need to develop rapid, sensitive, inexpensive and simple in use biosensor for the determination of GVA.

Advances in Zinc Oxide (ZnO) growth technology allow the formation of nanostructures with desired optical, structural, morphological and electrical properties that are exploited in the range of biosensors (Tereshchenko *et al.*, 2016; Yakimova *et al.*, 2012). Due to its high isoelectric point (~ 9.5), biocompatibility, high chemical stability, strong adsorption ability, high catalytic efficiency along with nontoxicity and abundance in nature, ZnO is suitable for the immobilization of biomaterials, which are applied as biological recognition parts in biosensors (Tereshchenko *et al.*, 2016; Yakimova *et al.*, 2012). As a wide and direct band gap (3.37 eV) semiconductor that has intense photoluminescence at room temperature, ZnO is widely applied in optical biosensors (Iyer *et al.*, 2014; Kang *et al.*, 2015; Picciolini *et al.*, 2015; Politi *et al.*, 2015b; Shukla *et al.*, 2015) particularly photoluminescence based biosensors (Elhag *et al.*, 2015; Sodzel *et al.*, 2015; Viter *et al.*, 2014). In this type of biosensors, the changes in the photoluminescence signal of nanostructured material are used for the detection of analyte and the determination of its amount by characterization of photoluminescence spectra. Therefore recently, a wide range of PL biosensors based on ZnO nanostructures have been developed (Elhag *et al.*, 2015; Sodzel *et al.*, 2015; Tereshchenko *et al.*, 2016; Viter *et al.*, 2014).

Among various methods used to form ZnO thin films, atomic layer deposition (ALD) is an innovative technique, which allows the deposition of ultrathin metal oxide films with controlled thickness, grain size, chemical composition, texture, surface morphology and defect concentration. The mentioned structural parameters make a strong impact on optical, electrical and mechanical properties (Chaaya *et al.*, 2013). In previous studies (Bechelany *et al.*, 2015;

Chaaya et al., 2013; Viter et al., 2015a, 2015b, 2016), we investigated the tuning of the optical and the structural properties of ultrathin ZnO films deposited by ALD along with their potential applications in sensors and biosensors (Chaaya et al., 2013).

In the wide range of studies, the influence of adsorption and immobilized proteins on the optical properties of ZnO was investigated (Elhag et al., 2015; Politi et al., 2015a, 2015b; Sodzel et al., 2015; Viter et al., 2012, 2014; Yan et al., 2012). The majority of results reports on the changes in photoluminescence intensity and peak positions of near band emission (NBE) and/or deep level emission (DLE) of ZnO after interaction with biomolecules. In rare cases, the immobilized proteins induce new photoluminescence peak or line on the spectra (Politi et al., 2015a, 2015b) but the photoluminescence caused by protein adsorption was not strong enough to be used as a biosensor response. In the present work, the influence of immobilized GVA-antibodies (**against GVA-antigens**) on the photoluminescence spectra of ZnO was investigated for the first time. The direct immobilization of **anti-GVA** antibodies on the ZnO surface was performed and resulted in **the formation of biosensing structure (ZnO/anti-GVA), which was characterized by increased** intensity of the main NBE peak of ZnO **and photoluminescence band appearance in the range around 425 nm**. The changes in the photoluminescence **of ZnO/anti-GVA caused by formation of complex between immobilized anti-GVA antibodies and GVA-antigens** were **interpreted as analytical signal**. Novel, label free and sensitive photoluminescence based biosensor for GVA-antigens has been developed.

## **2. Materials and Methods**

### **2.1. ZnO thin film synthesis and characterizations**

ZnO layers of 57 and 110 nm thicknesses were synthesized by ALD method using lab-made ALD reactor at the same conditions as described elsewhere. ALD was performed using

sequential exposures of Diethyl Zinc (DEZ) ( $\text{Zn}(\text{CH}_2\text{CH}_3)_2$ , 95% purity, CAS: 557-20-0) and  $\text{H}_2\text{O}$  separated by a purge of Argon with a flow rate of 100 sccm. The deposition regime for ZnO consisted of 0.2 s pulse of DEZ, 30 s of exposure and 30 s of purge with Argon followed by 2 s pulse of  $\text{H}_2\text{O}$ , 30 s of exposure to  $\text{H}_2\text{O}$  and finally 40 s purge with Argon. ZnO ultrathin films with different numbers of cycles were deposited at 100 °C.

## **2.2. Chemical and physical characterizations of ZnO thin films**

Structural properties of ZnO films were characterized by Scanning Electron Microscopy (SEM), Ellipsometry and Grazing Incidence X-ray Diffraction (GIXRD). Optical properties were characterized by photoluminescence (PL) study of ZnO films that was used further as a biosensor signal.

In order to investigate the photoluminescence of the studied samples, they were excited by a solid state laser with a wavelength of 355 nm. The excited ZnO PL entered a spectrometer with the slit entrance of 1 by 1 mm, a focal length of 550, a 600 gr/mm grating and a liquid nitrogen cooled CCD as the detector. The large, 0.4 mm wide, excitation area was produced in order to obtain an average PL of each sample. The spot size on the sample was a diameter of roughly 1 mm. The laser power was 1.2 mW. All PL experiments were recorded at room temperature, with a spectral resolution of 3.3 nm, using the spectrometer TRIAX 550 made by Jobin Yvon (New Jersey, USA). The laser was blocked by a 364 nm long pass filter after the sample, with full transmission from 368 nm.

## **2.3. Functionalization of ZnO thin films**

The biological samples used in the experiment were provided by National Scientific Centre “Institute of Viticulture and Wine Making named after V. Ye. Tairov” (Odessa, Ukraine).

The used proteins were part of the immunoassay-based KIT for the determination of GVA produced by Agritest (Valenzano, Italy) and consisted from anti-GVA antibodies containing serum, which in deed was a real sample extracted from GVA-infected grape plants; control sample of GVA antigens, containing extract of GVA-infected grape plants (further in the text it is marked as 'Ag+') and real sample of non-infected plant extract, which does not contain any proteins of GVA virus capsid (further in the text it is marked as 'Ag-'). The molecular weight of GVA capsid proteins, which were present in Ag+ sample is ~ 27 kDa (Monette and Green, 1992).

The anti-GVA antibody immobilization procedure was the following: 5 µl of anti-GVA antibodies containing sample was diluted by 50, 100, 200, 400, 600, 800, 1000 times that corresponds 1/50, 1/100, 1/200, 1/400, 1/600, 1/800, 1/1000 respectively, were dissolved in 0.01 mol/l PBS (pH=7.4) and this solution was equally distributed on the surface of as grown ZnO film modified substrates with the size 5\*5 mm, and it was kept for 1 hour in humid environment at room temperature. After this, the samples were washed with PBS and with deionized water and then they were dried in air for 1 hour at room temperature. By above mentioned procedure biosensing structure (ZnO/anti-GVA) was formed. After all, the PL signal of ZnO/anti-GVA was recorded.

#### **2.4. Evaluation of biosensor performance**

The procedure for the determination of GVA antigens was following: 5 µl of GVA antigens containing samples of different concentrations from 1 pg/ml to 1 µg/ml dissolved in 0.01 mol/l PBS (pH=7.4) and this solution was equally distributed on the surface of ZnO film modified substrates with the size 5×5 mm, and it was kept for 1 hour in humid environment at room temperature. After this, the samples were washed with PBS and with deionized water and then they were dried in air for 1 hour at room temperature. After all, the PL signal was recorded.

Before biosensor test, optical properties (absorbance and PL) of anti-GVA-based substrates were studied. The absorbance spectra were recorded with UV-VIS spectrophotometer Shimadzu UV-1700 (Kyoto, Japan) in the range of 250-600 nm. The PL spectra were registered using setup described above.

### 3. Results and Discussion

The SEM images of ALD ZnO thin films deposited on Si substrates with different numbers of cycles are represented in figure 1a. The SEM images show a conformal coating of the Si substrate by the ALD formed the ZnO films. With increasing thickness of ZnO films, a rough surface with columnar growth has been observed. Elipsometry-based measurements confirmed that ZnO film thickness of 57 and 110 nm (noted as ZnO<sub>57nm</sub> and ZnO<sub>110nm</sub>) were obtained respectively by 250 and 500 ALD cycles which correspond to a growth of 2.2 Å per one cycle. GIXRD diffraction patterns of ZnO thin films are shown in figure 1b. It demonstrates the diffraction peaks at  $2\theta = 31.80^\circ$ ,  $34.54^\circ$  and  $36.16^\circ$ , which are corresponding to (100), (002), and (101) reflection planes of hexagonal wurtzite structure of ZnO respectively.

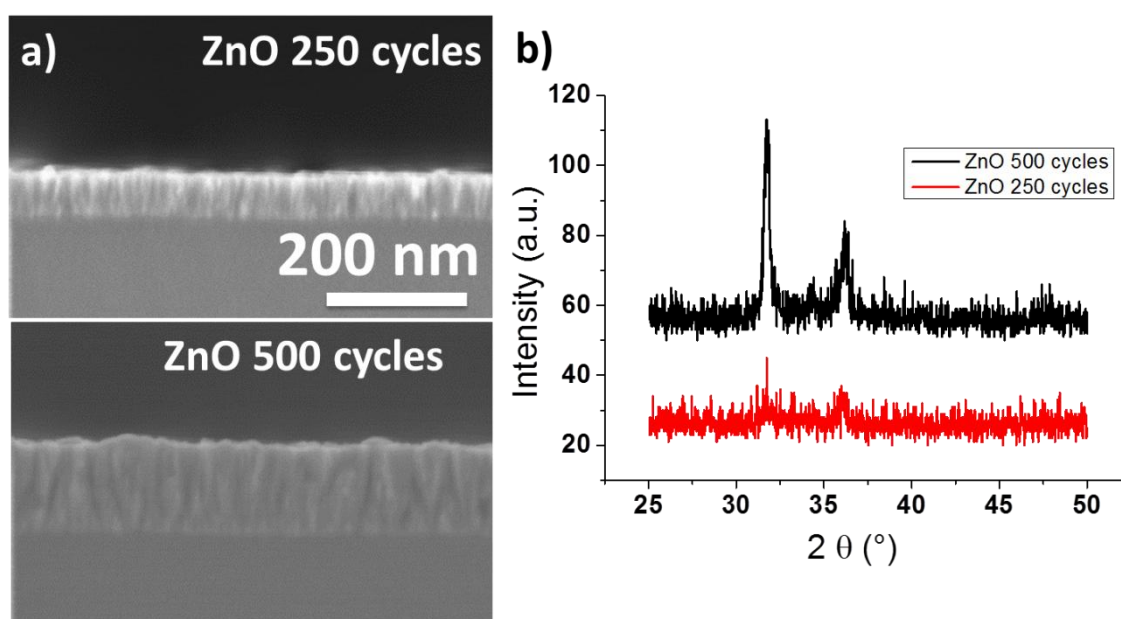
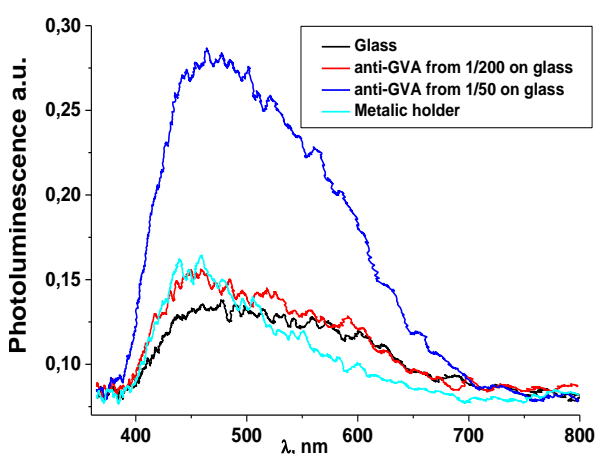
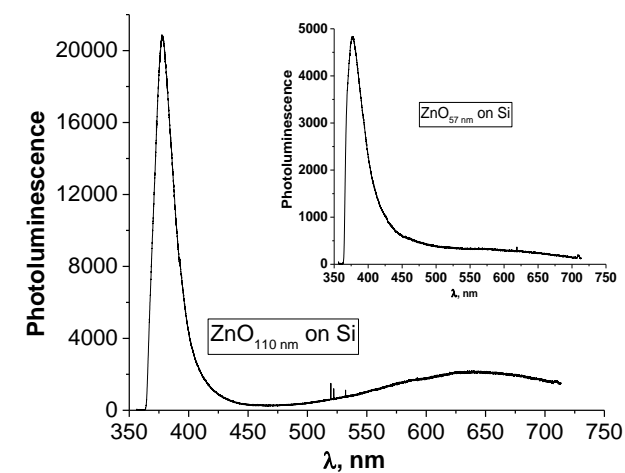




**Figure 1.** a) SEM cross section images and b) GIXRD of ZnO ALD films deposited on Si substrates by different numbers of cycles (250 and 500).

### 3.1. Photoluminescence-based characterization of ZnO films deposited on Si substrate

PL spectra of the samples were characterized by NBE peak at 378 nm (Fig. 2 a). The films with the layer thickness of 110 nm ( $\text{ZnO}_{110\text{nm}}$ ) demonstrate more intense NBE peak (as it was expected) and DLE emission in the visible range. At the same time,  $\text{ZnO}_{57\text{nm}}$  films are characterized by weak PL emission in the range around 450 nm (Fig. 2a, inset).



a)

b)

Figure 2. PL spectra of the ZnO samples with 57 and 110 nm layer thicknesses (a), PL spectra of anti-GVA deposited on glass (b).

### 3.2. Immobilization of anti-GVA on the surface of ZnO films

Among the large variety of biosensors, **immunosensors** are based on specific interaction between antibody – antigen couple (Iyer et al., 2014). The interaction between antibody and antigen couple has high specificity and sensitivity to detect analytes what makes **immunosensors** suitable for accurate and precise **analysis** with different types of transducers. Optical **transducers** are simple, fast and accurate, **therefore they are very suitable for the** detection of target analyte. **Out of many optical approaches,** photoluminescence based methods **are among the most sensitive and simple ones** (Politi et al., 2015a, 2015b; Sodel et al., 2015; Viter et al., 2012). **In PL-based sensors nanostructured** photoluminescent materials are often used as transducers due to their ability to convert molecular interactions **into PL-signals** without contamination or deterioration of the samples (Politi et al., 2015a). The principle of the PL-based biosensor action is based on the **changes** of PL signal before and after interaction **of immobilized bio-recognition sites** with analyte (Politi et al., 2015a; Sodel et al., 2015; Tereshchenko et al., 2016), see figure 3.

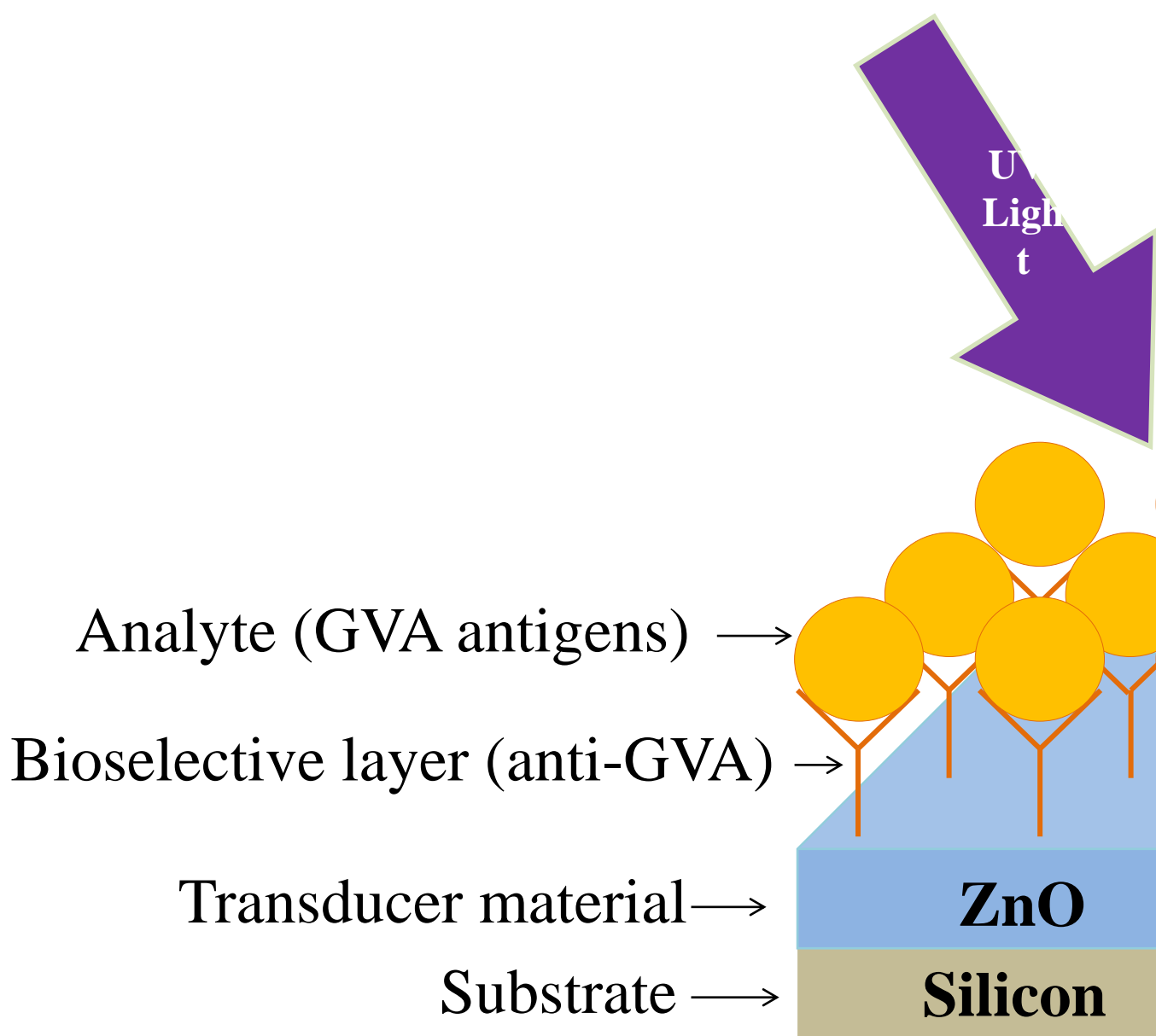


**Figure 3.** The scheme of PL based immunosensor.

In order to investigate the possibility of application of ZnO films, which were deposited by ALD method, as an optical transducer of immunosensor and to determine the optimal surface-concentration of anti-GVA antibodies immobilized in the biosensitive layer, anti-GVA solutions of different concentrations were deposited on the surface of ZnO-modified substrates. For both ZnO<sub>110nm</sub> and ZnO<sub>57nm</sub> samples, the immobilization of anti-GVA have resulted in appearance of PL band in the range from 400 to 550 nm along with the intensity increase of the NBE peak in

average by 35% (Fig. 4a). However, NBE peak shift was not observed and no significant difference in the PL spectra after immobilization of the same anti-GVA concentration on the surface of ZnO<sub>110nm</sub> and ZnO<sub>57nm</sub> modified substrates was observed (the spectra are not shown here). Therefore, the films with the layer thickness of 110 nm were chosen for the further immunosensor design.

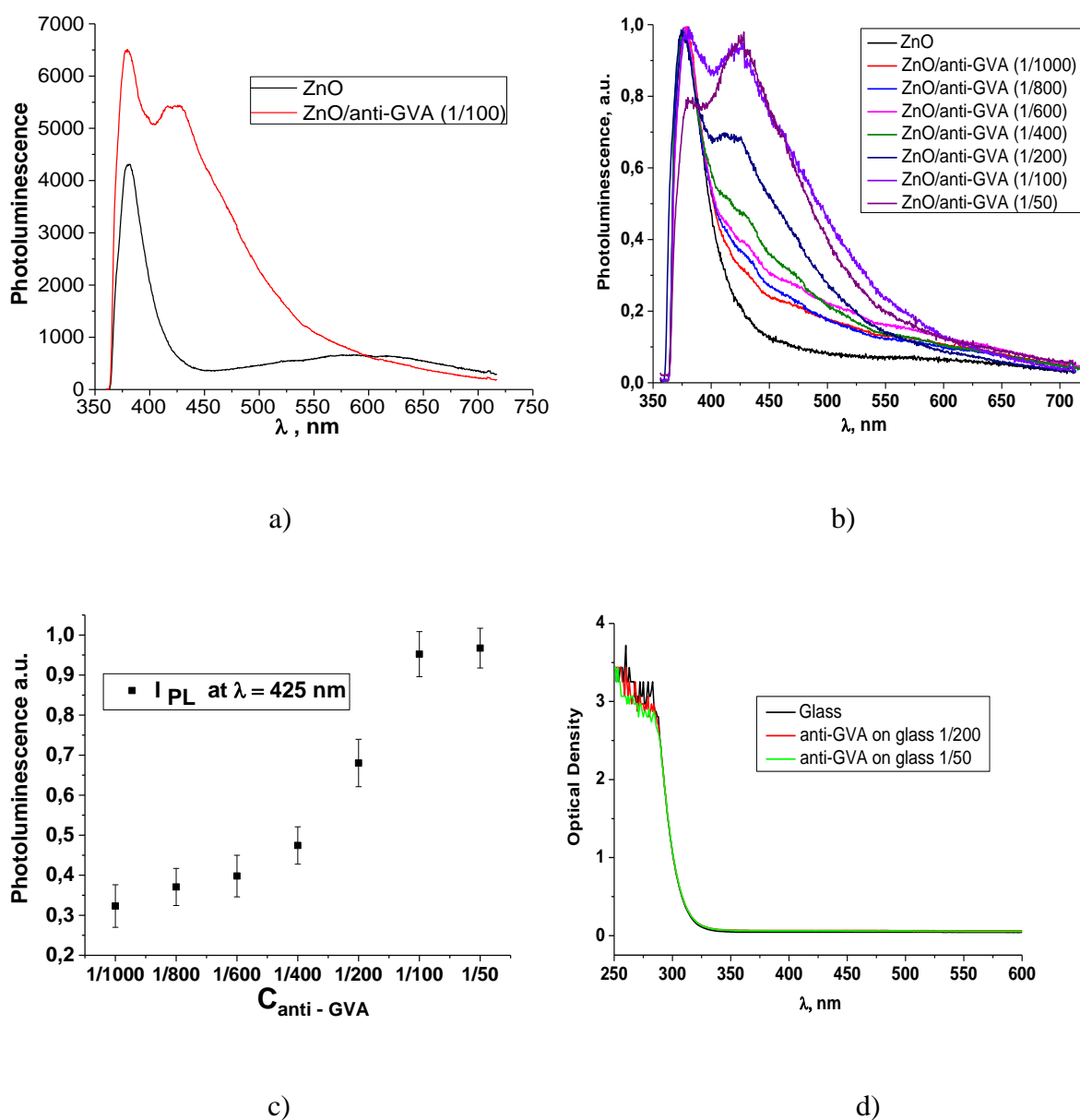


**Figure 4.** PL spectra of bare ZnO<sub>110nm</sub> and ZnO<sub>110nm</sub> functionalized with anti-GVA using 1/200 diluted solution (a), PL spectra of bare ZnO<sub>110nm</sub> and ZnO<sub>110nm</sub> functionalized with anti-GVA using solutions containing different concentrations of anti-GVA (b), PL intensity at 425 nm as a function of concentration of anti-GVA solutions used for the modification of ZnO-based

substrates (c), absorbance spectra of anti-GVA deposited on glass from two solutions containing different concentrations of anti-GVA antibodies (d).

Figure 4b presents the PL spectra of the  $\text{ZnO}_{110\text{nm}}$  films with immobilized anti-GVA antibodies ( $\text{ZnO}_{110\text{nm}}/\text{anti-GVA}$ ) from the solutions with different concentrations of anti-GVA, which are ranging from the lowest concentration (at 1/1000 dilution of initial anti-GVA containing solution) to the highest concentration (at 1/50 dilution). The initial PL signal intensity among all ZnO films was varying from 16000 to 19000 arbitrary units. Thus, the PL spectra (Fig. 4b) were normalized in order to eliminate the fluctuation of this varying initial signal and to compare the influence of protein adsorption on ZnO. Such immobilization of anti-GVA has resulted in the appearance of PL emission in the range from 400 to 550 nm. This intensity increases with the increase of surface-concentration of anti-GVA adsorbed from solutions containing different anti-GVA concentrations (Fig. 4b). For low surface-concentrations of anti-GVA (adsorbed from initial anti-GVA solutions diluted by 1/1000 to 1/400 times), the photoluminescence caused by protein adsorption looks like PL band, which intensity increases with anti-GVA surface-concentration. In the  $\text{ZnO}_{110\text{nm}}/\text{anti-GVA}$  films, which were formed by immobilization of anti-GVA from 1/200 diluted initial anti-GVA solution, the PL emission turns to the formation of PL peak, which is centered at 425 nm, with the intensity increasing proportionally to the immobilized anti-GVA surface-concentration. For the  $\text{ZnO}_{100\text{nm}}/\text{anti-GVA}$  films formed from the highest concentration (1/50 diluted initial anti-GVA sample) of anti-GVA containing sample, a redistribution of the peak intensities was observed between the PL peak attributed to the protein emission and the peak related to NBE of ZnO. The dependence of PL intensity vs anti-GVA concentration at the  $\lambda=425$  nm (protein attributed PL) is shown in figure 4c. This dependence indicates that the saturation of the PL signal of  $\text{ZnO}_{110\text{nm}}/\text{anti-GVA}$  films appears for the films formed from 1/100 diluted initial sample of anti-GVA. Therefore, the

optimal concentration of anti-GVA for the formation of biosensitive layer was in the 1/200 diluted sample.

Optical properties of anti-GVA were investigated by PL and absorbance measurements. The PL spectra of anti-GVA deposited on glass substrates are shown in figure 2b. No PL line around 425 nm was observed for the samples formed using solutions with highest anti-GVA concentrations from 1/200 and 1/50 diluted samples. The spectra of optical absorbance of the same samples (Fig. 4d) demonstrate that anti-GVA antibodies do not have optical activity by themselves in the UV-VIS range of spectra. Therefore, the PL line at 425 nm is caused by the luminescence, resulted from the interaction of anti-GVA with ZnO.

### 3.3. Performance of immunosensor

The sensitivity of immunosensor was tested using ZnO<sub>110nm</sub> film modified by anti-GVA from 1/200 diluted initial anti-GVA sample. The target analyte used in the experiment was GVA antigen (Ag<sup>+</sup>) that is specifically bounding to the anti-GVA, because both, anti-GVA and GVA antigen, are complementary to each other and by interaction they are forming an 'immune complex'. The concentration of Ag<sup>+</sup> was in the range from 1 pg/ml to 1 µg/ml (Fig. 5a). The interaction between ZnO<sub>110nm</sub>/anti-GVA and GVA antigen, which is present in Ag<sup>+</sup> sample, resulted in the decrease of the NBE peak intensity by 20 % in average for all ZnO<sub>110nm</sub>/anti-GVA/Ag<sup>+</sup>-based structures. However, the initial variation of NBE peak intensity for all ZnO<sub>110nm</sub> samples disabled the application of NBE intensity changes as a sensor signal. Therefore, the spectra were normalized and the response of the biosensor was based on the change in the intensity of PL band at 425 nm corresponding to the luminescence of anti-GVA (Fig. 5a). The response of the as formed immunosensor was observed at the Ag<sup>+</sup> concentrations from 1 pg/ml to 10 ng/ml, where the intensity of protein related PL line decreased with the

increase of the Ag<sup>+</sup> concentration (Fig. 6). The further increase of the Ag<sup>+</sup> concentrations led to the **increasing** PL intensity and full saturation of the PL signal at the 1 µg/ml.

The biosensor response ( $S$ ) was calculated using the equation 1 (Sodzel et al., 2015; Viter et al., 2012, 2014):

$$S = \frac{I_{Ab} - I_{Ab-Ag}}{I_{Ab}}; \quad (1)$$

where  $I_{Ab}$  is a PL intensity at 425 nm of ZnO<sub>110nm</sub> with immobilized anti-GVA;  $I_{Ab-Ag}$  is the PL intensity at 425 nm of ZnO<sub>110nm</sub> with immobilized anti-GVA and GVA antigen (Ag).

The sensitivity of obtained biosensor to the GVA Ag<sup>+</sup> is in the range from 1 pg/ml to 10 ng/ml (Fig. 6, inset).

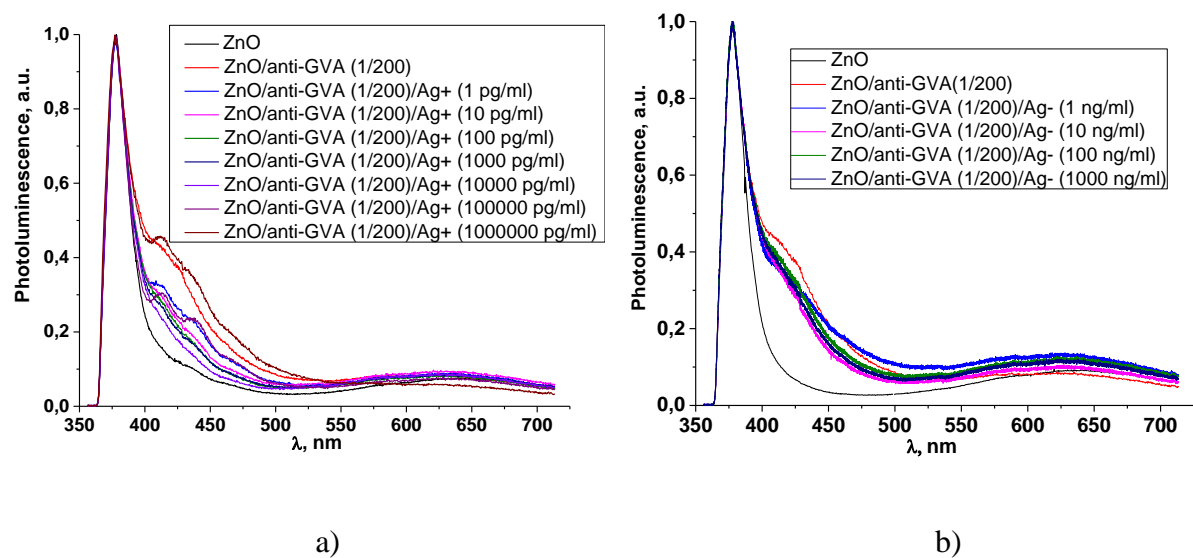


**Figure 5.** The dependence of ZnO<sub>100nm</sub>/anti-GVA/Ag<sup>+</sup> PL spectra after incubation of ZnO<sub>100nm</sub>/anti-GVA-based immunosensor in different antigen concentrations containing specimens (specimens – Ag<sup>+</sup>) (a), PL spectra dependence of ZnO<sub>100nm</sub>/anti-GVA-based immunosensor under different concentrations of proteins separated from healthy vine plants, which not contains antigen for anti-GVA (specimens – Ag<sup>-</sup>) (b).

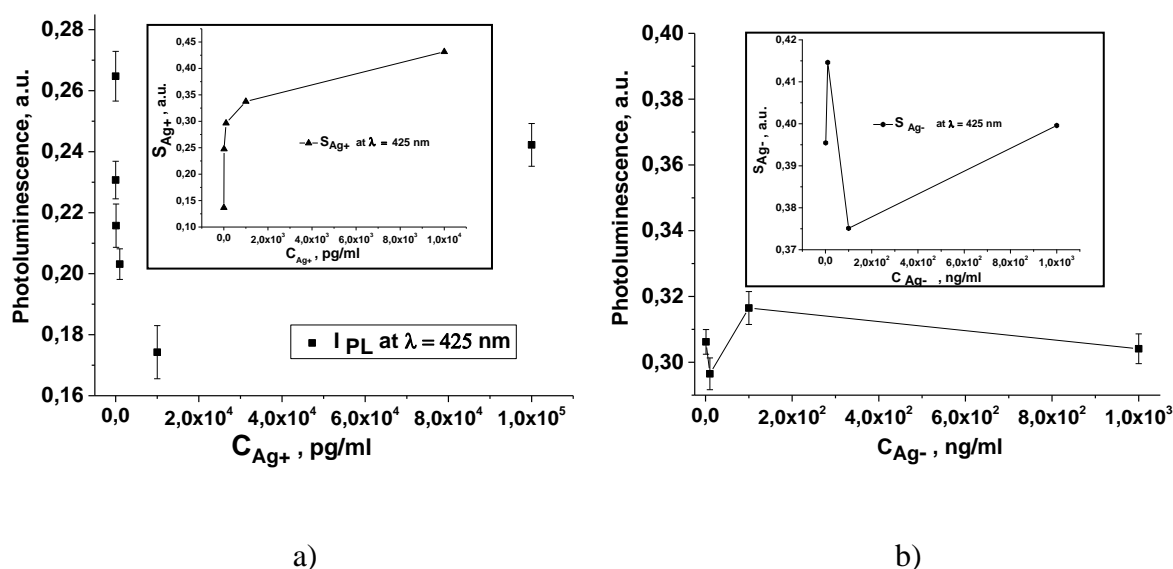


**Figure 6.** PL intensity at 425 nm as a function of GVA antigen concentration in Ag+ specimen, inset – biosensor response ( $S$ ) as a function of GVA antigen concentration in Ag+ specimen (a), PL intensity at 425 nm as a function of different concentrations of proteins separated from healthy vine grapes, which not contain antigen for anti-GVA (specimens – Ag-), inset - biosensor response ( $S$ ) as a function of Ag- specimen concentration (b).

The sensitivity of here proposed immunosensor cannot be compared directly with the one of already known and widely applied methods for GVA antigen detection, which are based on enzyme linked immune-sorbent assay (ELISA) or real time polymerase chain reaction (RT-PCR) tests. Both (ELISA and RT-PCR) methods are providing very efficient detection of GVA, which is close to 100%, but these methods are based on number of chemical/biochemical reactions and another analytical signal detection principles. Therefore both (ELISA and RT-PCR) methods in comparison with action of here proposed immunosensor are time-consuming, needs initial sample preparation and requires much more advanced equipment. In addition by both (ELISA and RT-PCR) methods the quantitative determination of concentration of GVA antigens is not very easy and is technically complicated. The detection of GVA antigens using optical properties of ZnO film formed by ALD method proved to be relatively sensitive and selective analytical



approach, which could be characterized as an express **method, because** it does not involve the application of **additional labels, such as enzymes, which are used in ELISA, fluorescent-dyes, which are used in RT-PCR.** Therefore here proposed immunosensor is **simpler in use** and much cheaper as well.

In order to check the selectivity of the biosensor, the **control specimen – Ag-, which was isolated from the non-infected grapevine plants and not contained any GVA proteins, was deposited and incubated on the biosensitive layer of immunosensor that was formed using 1/200 diluted sample of initial anti-GVA sample.** Therefore in the latest specimen no proteins that could specifically bound to the anti-GVA were present. The **incubation of ZnO/anti-GVA-based immunosensor with control-specimen Ag-** resulted in the decrease of NBE peak intensity and PL emission in the region of 400-500 nm (Fig. 5b). However, unlike the case of **Ag+ specimen, PL lines, which are related to the GVA emission, have overlapped with each other and intersected at wavelength around 425 nm.** Unlike the covalent binding, which is known as a “strong” binding between protein and substrate that provides a significant structure of the bioselective layer and improves the biorecognition, however it involves a cross-linking agent between ZnO surface and molecules of the bioselective layer, which significantly complicates the general procedure, increases the cost of the experiment and partly damages immobilized antibodies. Therefore, in the absence of GVA antigens no **specific** biosensor response was observed (Fig. 6b).

In the case of direct **adsorption** of biosensitive layer (anti-GVA **antibodies**) the binding between ZnO and biomolecules occurs due to Van der Waals forces and hydrogen bonds (Tereshchenko et al., 2016; Viter et al., 2014). The increase of PL intensity of NBE peak after the formation of biosensitive layer results from the charge transfer between anti-GVA molecules and conductance band of ZnO (Politi et al., 2015a, 2015b; Tereshchenko et al., 2016; Viter et al., 2012, 2014). The phenomenon is known as an adsorption assisted increase of exciton-phonon interaction, which is evident from the change of NBE-related peak of ZnO. After

'biofunctionalization' of ZnO thin film surface, the PL emission increases since the molecular complexes can supply extra free electrons, which can participate in transitions between different surface energy levels (Politi et al., 2015a).

The quenching of the main ZnO peak and the decreasing of PL intensity related to anti-GVA antibodies (which are proteins) after **their interaction with** target-analyte (**GVA antigen**), which is present in Ag<sup>+</sup> specimen, may be **induced by** several reasons. The surface reaction with a quencher may introduce non-radiative surface defects. In addition, the charge transfer from a radiative material to a quencher can also be one of the main mechanisms of the PL quenching (Tereshchenko et al., 2016). Sodzel *et al.* have suggested the collisional PL quenching mechanism, responsible for the recognition of the analyte. Under laser excitation, the carriers in ZnO are separated into conduction band (CB-electrons) and valence band (VB-holes). The carriers aim to recombine radiatively while emitting a photon with energy close to the ZnO band gap (~3.3 eV) for NBE emission or alternatively through the level defects with energies ~2.9 eV for the protein related emission (Sodzel et al., 2015).

The appearance of protein related luminescence band in the range of 400-500 nm can be caused by radiative transitions from defect states in the forbidden gap to valence band of ZnO. Zn interstitial states (~2.97 eV (Dumcenco et al., 2012; Zhao and Jiang, 2010)) and Zn vacancies (3.09 eV (Sodzel et al., 2015)) can play the role of adsorption centers of immobilized proteins. From the other side, the increase of PL peak at 425 nm, which is observed at high concentrations of anti-GVA antibodies, is in the same region as the blue emission peak of ZnS (Ramanavicius et al., 2009; Wang et al., 2013). This fact indicates that during the adsorption process the disulfide bonds, which are formed between the chains of anti-GVA, at least partly dissociates (Balevicius et al., 2011; Baleviciute et al., 2013; Baniukevic et al., 2013a, 2013b; Kausaite-Minkstimiene et al., 2013; Makaraviciute et al., 2014) and forms strong complexes (-O-Zn-S-anti-GVA) with Zn atoms, which are present in ZnO structure. The quenching of both NBE (378 nm) and protein

related (425 nm) PL peaks after antigen-antibody interaction of ZnO/anti-GVA with target analyte can be related to the partial elimination and/or weakening of interactions between anti-GVA and ZnO, which were formed during the immobilization of anti-GVA molecules on the ZnO surface.

#### 4. Conclusions

Optical properties of ZnO films obtained by ALD method were applied for the detection of GVA antigens for the first time. The detection of GVA antigens was performed through direct immobilization of anti-GVA **antibodies** on the ZnO thin film surface, forming the biosensitive layer. The immobilization of anti-GVA **antibodies** resulted in new PL band appearance in the region 400-550 nm that can be caused by the formation of ZnS compound during the adsorption process. The GVA antigen detection was performed using the changes in the GVA related PL band behavior. The sensitivity of obtained biosensor is in the range **from 1 pg/ml to 10 ng/ml of protein**. The biosensor selectivity has been proved by test based on application of **control specimen – Ag, which was isolated from the non-infected grapevine plants and not contained any GVA proteins (antigens)**.

The possibility **to detect GVA antigens without additional labels (e.g enzymes, which are used in ELISA, or fluorescent dyes, which are used in RT-PCR)** has been demonstrated. The decrease of the deposition time of immobilized layers has been achieved. The general duration of the experiment procedure **is few times shorter than ELISA and RT-PCR**. **Due to good performance and simplicity of here described immunosensor ZnO-modified substrates could be applied as a platform for the development of other immunosensors based on immobilized antibodies, which would be sensitive to selected analyte.**

## 5. Acknowledgment

This work was supported by EU grant under BIOSENSORS-AGRICULT, Contract PIRSES-GA-2012-318520 “Development of nanotechnology based biosensors for agriculture”.

## 6. References

- Balevicius, Z., Ramanaviciene, A., Baleviciute, I., Makaraviciute, A., Mikoliunaite, L., Ramanavicius, A., 2011. *Sensors and Actuators B: Chemical* 160(1), 555-562.
- Baleviciute, I., Balevicius, Z., Makaraviciute, A., Ramanaviciene, A., Ramanavicius, A., 2013. *Biosensors and Bioelectronics* 39(1), 170-176.
- Baniukevic, J., Boyaci, I.H., Bozkurt, A.G., Tamer, U., Ramanavicius, A., Ramanaviciene, A., 2013a. *Biosensors and Bioelectronics* 43, 281-288.
- Baniukevic, J., Kirlyte, J., Ramanavicius, A., Ramanaviciene, A., 2013b. *Sensors and Actuators B: Chemical* 189, 217-223.
- Bechelany, M., Balme, S., Miele, P., 2015. *Pure and Applied Chemistry* 87(8), 751-758.
- Chaaya, A.A., Viter, R., Bechelany, M., Alute, Z., Erts, D., Zaleskaya, A., Kovalevskis, K., Rouessac, V., Smyntyna, V., Miele, P., 2013. *Beilstein Journal of Nanotechnology* 4, 690-698.
- Du Preez, J., Stephan, D., Mawassi, M., Burger, J.T., 2011. *Archives of Virology* 156(9), 1495-1503.
- Dumcenco, D., Huang, Y., Kuo, D., Tiong, K., 2012. *Journal of Luminescence* 132(8), 1890-1895.
- Elhag, S., Ibutoto, Z.H., Khranovskyy, V., Willander, M., Nur, O., 2015. *Vacuum* 116, 21-26.
- Goszczynski, D.E., 2014. *Archives of Virology* 159(9), 2523-2528.
- Iyer, M.A., Oza, G., Velumani, S., Maldonado, A., Romero, J., Munoz, M.d.L., Sridharan, M., Asomoza, R., Yi, J., 2014. *Sensors and Actuators B: Chemical* 202, 1338-1348.
- Kang, Z., Gu, Y., Yan, X., Bai, Z., Liu, Y., Liu, S., Zhang, X., Zhang, Z., Zhang, X., Zhang, Y., 2015. *Biosensors and Bioelectronics* 64, 499-504.
- Kausaite-Minkstimiene, A., Ramanavicius, A., Ruksnaite, J., Ramanaviciene, A., 2013. *Analytical Methods* 5(18), 4757-4763.
- Makaraviciute, A., Ruzgas, T., Ramanavicius, A., Ramanaviciene, A., 2014. *Analytical Methods* 6(7), 2134-2140.
- Misbeh, S., Al-Musa, A., Anfoka, G., Salem, N., 2007. *Phytopathologia Mediterranea* 46(2), 195-200.
- Monette, P., Green, M., 1992. *Canadian Journal of Plant Pathology* 14(4), 267-270.
- Picciolini, S., Castagnetti, N., Vanna, R., Mehn, D., Bedoni, M., Gramatica, F., Villani, M., Calestani, D., Pavesi, M., Lazzarini, L., 2015. *RSC Advances* 5(113), 93644-93651.
- Politi, J., Gioffrè, M., Rea, I., De Stefano, L., Rendina, I., 2015a. *SPIE Optics+ Optoelectronics*, pp. 95061Z-95061Z-95067. International Society for Optics and Photonics.
- Politi, J., Rea, I., Dardano, P., De Stefano, L., Gioffrè, M., 2015b. *Sensors and Actuators B: Chemical* 220, 705-711.
- Ramanavicius, A., Karabanovas, V., Ramanaviciene, A., Rotomskis, R., 2009. *Journal of Nanoscience and Nanotechnology* 9(3), 1909-1915.
- Shukla, S., Sharma, N.K., Sajal, V., 2015. *Sensors and Actuators B: Chemical* 206, 463-470.
- Sodzel, D., Khranovskyy, V., Beni, V., Turner, A.P., Viter, R., Eriksson, M.O., Holtz, P.-O., Janot, J.-M., Bechelany, M., Balme, S., 2015. *Microchimica Acta* 182(9-10), 1819-1826.
- Tereshchenko, A., Bechelany, M., Viter, R., Khranovskyy, V., Smyntyna, V., Starodub, N., Yakimova, R., 2016. *Sensors and Actuators B: Chemical*.

- Viter, R., Balevicius, Z., Abou Chaaya, A., Baleviciute, I., Tumenas, S., Mikoliunaite, L., Ramanavicius, A., Gertnere, Z., Zalesska, A., Vataman, V., Smyntyna, V., Erts, D., Miele, P., Bechelany, M., 2015a. *Journal of Materials Chemistry C* 3(26), 6815-6821.
- Viter, R., Chaaya, A.A., Iatsunskyi, I., Nowaczyk, G., Kovalevskis, K., Erts, D., Miele, P., Smyntyna, V., Bechelany, M., 2015b. *Nanotechnology* 26(10), 105501.
- Viter, R., Iatsunskyi, I., Fedorenko, V., Tumenas, S., Balevicius, Z., Ramanavicius, A., Balme, S., Kempniński, M., Nowaczyk, G., Jurga, S., Bechelany, M., 2016. *The Journal of Physical Chemistry C* 120(9), 5124-5132.
- Viter, R., Khranovskyy, V., Starodub, N., Ogorodniichuk, Y., Gevelyuk, S., Gertnere, Z., Poletaev, N., Yakimova, R., Erts, D., Smyntyna, V., 2014. *Sensors Journal, IEEE* 14(6), 2028-2034.
- Viter, R., Smyntyna, V., Starodub, N., Tereshchenko, A., Kusevitch, A., Doychoa, I., Geveluk, S., Slisshik, N., Buk, J., Duchoslav, J., 2012. *Procedia Engineering* 47, 338-341.
- Wang, J., Jiao, Y., Liu, Y., Zhang, Z., Qu, F., Wu, X., 2013. *Journal of Nanomaterials* 2013, 1.
- Yakimova, R., Selegård, L., Khranovskyy, V., Pearce, R., Lloyd Spetz, A., Uvdal, K., 2012. *Frontiers in bioscience (Elite edition)* 4(1), 254-278.
- Yan, X., Huang, Z., He, M., Liao, X., Zhang, C., Yin, G., Gu, J., 2012. *Colloids and Surfaces B: Biointerfaces* 89, 86-92.
- Zhao, Y., Jiang, Y., 2010. *Spectrochimica Acta Part A: Molecular and Biomolecular Spectroscopy* 76(3), 336-340.